Int. J. Solids Structures Vol. 20, No. 1, pp. 1–11, 1984
Printed in Great Britain.

0020-7683/84 $3.00 + .00

TORSION OF A LONG CYLINDRICAL ELASTIC BAR PARTIALLY EMBEDDED IN A LAYERED ELASTIC HALF SPACE

P. KARASUDHI, R. K. N. D. RAJAPAKSE and B. Y. HWANG
Division of Structural Engineering and Construction, Asian Institute of Technology, P.O. Box 2754, Bangkok, Thailand

(*Received* 26 *August* 1982; *in revised form* 28 *April* 1983)

Abstract—This is a study of the axially symmetric torsion of a long elastic cylindrical bar which is embedded in a layered elastic half space. The stress singularity factor at the embedded end of the bar is estimated by an existing method, and its effects on the solution are investigated. Such effects are found to be not so significant, especially for long bars and when the main concern is only on the torque-twist angle relationship. Even for rather short bars, the results given by this study agree well with those by an existing method, which is more rigorous but restrictive only to the case of an infinitely rigid bar.

1. INTRODUCTION

The main objective of this study is to develop a simple but efficient solution scheme for the problem of the axially symmetric torsion of an elastic cylindrical bar partially embedded in a layered elastic half space. The singularity factor for the shear stress along the base perimeter of the bar is estimated first by Williams' method[1]. The problem of an infinitely rigid bar partially embedded in a layered half space was solved by Luco[2]. Earlier, Freeman and Keer[3] solved the case of an elastic bar welded to the free surface of a homogeneous half space. In 1970, Keer and Freeman[4] solved the problem of a homogeneous half space and an elastic bar. The embedded part of the bar in Ref.[4] is infinitely long, while the unembedded part is finite. The problem of a homogeneous elastic half space containing an axially-loaded rigid bar was solved by Luk and Keer[5] in 1979.

Following the scheme proposed by Muki and Sternberg[6] for the treatment of the problem of an axially loaded rod partially embedded in an elastic half space, the system of the present study depicted in Fig. 1 is decomposed into an extended half space and a fictitious bar as shown in Figs. 2(a, b). Based on an appropriate compatibility condition between the two latter systems, which is different from that used in Ref.[6], the problem is found to be governed by a Fredholm integral equation of the second kind. The torque transfer and the torque-twist angle relationship can be obtained numerically for various slenderness ratios of the bar and two ratios among shear moduli involved.

2. AXISYMMETRIC TORSION OF ELASTIC HALF SPACE

For the axially symmetric torsion of an elastic half space, the most efficient coordinates to be used are cylindrical coordinates r, θ and z, with z normal to the free surface of the half space. Due to the symmetry of the problem, functions involved are independent of θ and the

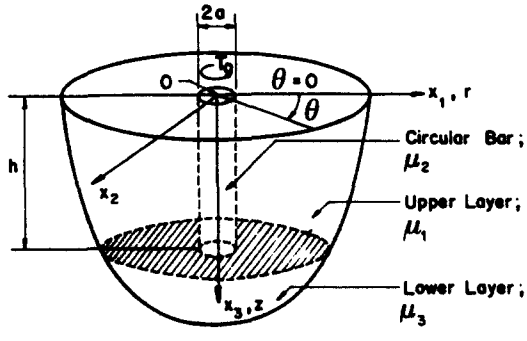

Fig. 1. Geometry of bar and embedding medium.

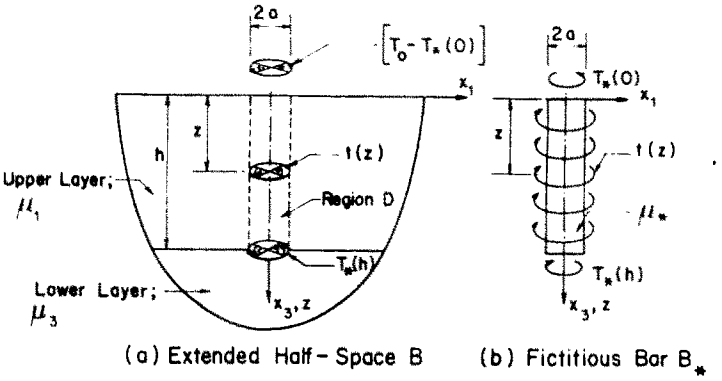

Fig. 2. Composition of the problem.

only non-trivial equilibrium equation is[7]

$$\frac{\partial^2 v}{\partial r^2} - \frac{v}{r^2} + \frac{\partial v}{r\partial r} + \frac{\partial^2 v}{\partial z^2} = 0 \tag{1}$$

where v is the displacement in θ direction, and the only displacement that remains nonzero. The nonvanishing components of stress are $\sigma_{\theta z}$ and $\sigma_{r\theta}$ which are related to v through the equations

$$\sigma_{\theta z} = \mu(\partial v/\partial z),\ \sigma_{r\theta} = \mu(\partial v/\partial r - r^{-1}v) \tag{2a,b}$$

where μ is the shear modulus of the medium.

The general solution to eqn (1) can be obtained by means of the technique of Hankel transform with respect to the radial coordinate as proposed by Muki[8] for elastostatics. Accordingly, the displacement v can be expressed as

$$v(r, z) = \int_0^\infty \xi^2 J_1(\xi r)(A\, e^{\xi z} + B\, e^{-\xi z})\, d\xi \tag{3}$$

where J_1 is the Bessel function of the first kind of the first order, and A and B are constants of integration to be determined from appropriate boundary and continuity conditions.

For reasons of convenience, it is appropriate to non-dimensionalise the problem by defining a, which denotes the radius of the embedded bar, as a unit of length.

3. ESTIMATION OF STRESS SINGULARITY FACTOR

It has been found by Luco[2], in the problem of torsion of a rigid cylindrical bar partially embedded in a layered elastic half space as shown in Fig. 1, that the shear stresses at the base perimeter of the bar are in the following singular forms

$$\sigma_{\theta z}(r, h) \sim r(1 - r^2)^{k-(1/2)},\ \sigma_{r\theta}(1, z) \sim [1 - (z/h)^2]^{k-(1/2)} \tag{4a,b}$$

where k is the stress singularity factor in the range $0 \leq k < 1/2$.

For the current problem of an elastic bar, the stress singularity factor can be taken as a function $k(\beta_1, \beta_2)$ where

$$\beta_1 = \mu_1/\mu_2,\ \beta_2 = \mu_1/\mu_3$$

in which μ_1 and μ_3 are the shear moduli of the upper and lower layers of the half space respectively, and μ_2 of the elastic bar. The method of Williams[1] can be applied to estimate the stress singularity by considering an analogous antiplane system, as shown in Fig. 3, consisting of two quarter planes with shear moduli μ_1 and μ_2 and a half plane with a shear modulus μ_3. Procedures similar to those of Ref.[4] will be used here. Adopting a reference coordinate

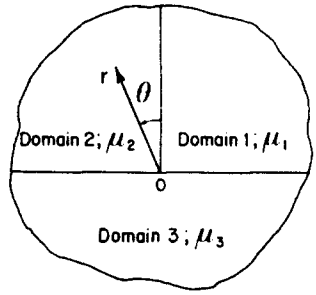

Fig. 3. Geometry of analogous antiplane system for estimating stress singularity factor.

system as shown in the figure, the only non-trivial equilibrium equation becomes

$$\frac{\partial^2 w_i}{\partial r^2} + \frac{1}{r}\frac{\partial w_i}{\partial r} + \frac{1}{r^2}\frac{\partial^2 w_i}{\partial \theta^2} = 0 \tag{6}$$

where the subscript i denotes a domain 1, 2 or 3 in the material system (Fig. 3), and w is the displacement in z direction and the only displacement that remains nonzero. The solution to eqn (6) can be put in the form

$$w_i(r, \theta) = r^{\lambda}[A_i \sin(\lambda\theta) + B_i \cos(\lambda\theta)] \tag{7}$$

where $\lambda = (2k+1)/2$, and A_i and B_i are arbitrary constants. The nonvanishing components of stress, $\sigma_{\theta zi}$ and σ_{zri}, are related to w_i through the equations

$$\sigma_{\theta zi}(r, \theta) = \mu_i r^{-1}\partial w_i/\partial\theta, \quad \sigma_{zri}(r, \theta) = \mu_i \partial w_i/\partial r. \tag{8a,b}$$

The continuity conditions appropriate for the present problem are

$$w_1(r, 0) = w_2(r, 0), \qquad \sigma_{\theta z1}(r, 0) = \sigma_{\theta z2}(r, 0) \tag{9a,b}$$

$$w_2(r, \pi/2) = w_3(r, \pi/2), \qquad \sigma_{\theta z2}(r, \pi/2) = \sigma_{\theta z3}(r, \pi/2) \tag{9c,d}$$

$$w_3(r, 3\pi/2) = w_1(r, 3\pi/2), \qquad \sigma_{\theta z3}(r, 3\pi/2) = \sigma_{\theta z1}(r, 3\pi/2). \tag{9e,f}$$

Substituting eqn (7) into eqns (9), in view of eqns (8), leads to a set of six homogeneous equations. For non-trivial solution of the arbitrary constants A_1 to A_3 and B_1 to B_3, the determinant of the coefficient matrix of this set of equations must be set to zero, i.e. after some manipulations,

$$\begin{vmatrix} \sin(\lambda_1) & -\sin(\lambda_1) & \cos(\lambda_1) & -\cos(\lambda_1) \\ \beta_2\cos(\lambda_1) & -\cos(\lambda_1) & -\beta_2\sin(\lambda_1) & \sin(\lambda_1) \\ -\beta_1\sin(3\lambda_1) & \sin(3\lambda_1) & -\cos(3\lambda_1) & \cos(3\lambda_1) \\ -\beta_1\cos(3\lambda_1) & \dfrac{\beta_1}{\beta_2}\cos(3\lambda_1) & \sin(3\lambda_1) & -\dfrac{\beta_1}{\beta_2}\sin(3\lambda_1) \end{vmatrix} = 0 \tag{10}$$

where $\lambda_1 = (2k+1)\pi/4$. The stress singularity factor $k(\beta_1, \beta_2)$ is the smallest positive real root of eqn (10) and less than 0.5. In general, a trial-and-error process has to be adopted to determine such a root. For some values of β_1 and β_2, the stress singularity does not even exist.

For the case of an infinitely rigid bar ($\beta_1 = 0$), eqn (10) can be reduced into

$$\sin\frac{3(2k+1)\pi}{4}\left[\sin k\pi - \frac{\beta_2}{1+\beta_2}\right] = 0 \tag{11}$$

from which the stress singularity factor can be readily obtained as

$$k(0, \beta_2) = \frac{1}{\pi} \arcsin \frac{\beta_2}{1+\beta_2}, \quad (0 \leqslant \beta_2 \leqslant 1) \tag{12a}$$

$$= \frac{1}{6}, \qquad (\beta_2 \geqslant 1). \tag{12b}$$

Equation (12a) agrees with the finding of Luco[2].

For a homogeneous half space ($\beta_2 = 1$), eqn (10) can be reduced to

$$(1-\beta_1) \sin \frac{3(2k+1)\pi}{4} = 0 \tag{13}$$

from which we get

$$k(\beta_1, 1) = \frac{1}{6}. \tag{14}$$

Thus the stress singularity factor for the case of an elastic bar embedded in a homogeneous half space is the same as that of an infinitely rigid bar embedded in a layered half space with $\beta_2 \geqslant 1$.

4. FUNDAMENTAL SOLUTION

At this stage, it is appropriate to consider the case of a shearing traction equivalent to a unit torque acting over a circular area of radius a in the interior of a layered elastic half space at $z = z'$ as shown in Fig. 4. This solution, which would serve as the fundamental solution necessary for solving the main problem, can be approached by considering the half space as divided into three domains, namely, domain 1 ($0 \leqslant z \leqslant z'$), domain 2 ($z' \leqslant z \leqslant h$) and domain 3 ($h \leqslant z < \infty$) as shown. The solution of each domain is in the form of eqn (3), containing two constants of integration A_i and B_i. The subscript i is used to denote a domain number. However, the constant A_3 should vanish to guarantee the boundedness of the solution as z approaches infinity. Thus there are five constants to be determined from the following boundary and continuity conditions:

$$\sigma_{\theta z 1}(r, 0) = 0 \tag{15a}$$

$$v_1(r, z') = v_2(r, z') \tag{15b}$$

$$v_2(r, h) = v_3(r, h) \tag{15c}$$

$$\sigma_{\theta z 2}(r, h) = \sigma_{\theta z 3}(r, h) \tag{15d}$$

$$\sigma_{\theta z 1}(r, z') - \sigma_{\theta z 2}(r, z') = \begin{cases} -2r/\pi, & (r < 1) \\ 0, & (r > 1) \end{cases} \tag{16a, 16b}$$

$$= -\frac{2}{\pi} \int_0^\infty J_1(\xi r) J_2(\xi)\, d\xi, \quad (0 \leqslant r < \infty). \tag{16c}$$

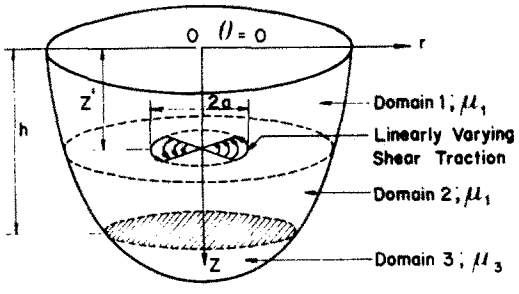

Fig. 4. Unit torque in the interior of layered half space.

To incorporate the notion of the singularity of the stress field in the form of eqns (4) at the base perimeter of a cylindrical bar of a radius a and length h embedded in the half space; the applied shear traction in the fundamental solution for $z' = h$ should be, in place of the linear eqn (16), in the form

$$\sigma_{\theta z1}(r, h) - \sigma_{\theta z3}(r, h) = \begin{cases} -\dfrac{(k+1/2)(k+3/2)}{\pi} r(1-r^2)^{k-(1/2)}, & (r<1) \quad (17a) \\ 0, & (r>1) \quad (17b) \end{cases}$$

$$= -2^{k-(1/2)}\Gamma(k+1/2)\frac{(k+1/2)(k+3/2)}{\pi}\int_0^\infty \xi^{-k+(1/2)} \times J_1(\xi r)J_{k+(3/2)}(\xi)\,d\xi, \quad (0 \leq r < \infty) \quad (17c)$$

and other two pertinent conditions are

$$\sigma_{\theta z1}(r, 0) = 0 \quad (18a)$$

$$v_1(r, h) = v_3(r, h). \quad (18b)$$

Note that, in this case, domain 2 does not exist, and there remain only three constants of integration, i.e. A_1, B_1 and B_3 to be determined by means of eqns (17c), (18a) and (18b). In eqn (17c), Γ denotes a gamma function.

5. TORSION OF ELASTIC CYLINDER EMBEDDED IN ELASTIC HALF SPACE

The problem of the axially symmetric torsion of an elastic cylindrical bar partially embedded in a layered elastic half space is depicted in Fig. 1. In addition to those previously defined, the following notations are introduced in this system; h denotes the depth of the bar and also the depth of the top layer; T_0 denotes the magnitude of the torque applied at the top end of the bar which is flush with the surface of the half space; and x_1, x_2 and x_3 are cartesian components of position vector $\mathbf{x}$; thus x_1 is identical to r for $\theta = 0$, and x_3 is identical to z. The top layer ($r > a$, $0 < z < h$) and the bottom layer ($z > h$) are perfectly bonded on the contact surface ($r > a$, $z = h$). The cylinder is bonded to the half space in the area ($r < a$, $z = h$) and along the surface of the cylinder ($r = a$, $0 \leq z \leq h$).

Following the approximative scheme similarly used by Muki and Sternberg[6] in the elastostatic axial load transfer, the system in Fig. 1 is decomposed into two systems; an extended half space B as shown in Fig. 2(a) and a fictitious bar B_* as shown in Fig. 2(b) with a shear moduli μ_* equal to the difference between the shear moduli of the real bar μ_2 and the half space μ_1, i.e.

$$\mu_* = \mu_2 - \mu_1 \geq 0. \quad (19)$$

The extended half space is subjected to a distributed bond torque $t(z)$ which is exerted by B_* on B at $x_3 = z$ in a region D in place of the bar. In addition, B is also subjected to end torques $T_0 - T_*(0)$ and $T_*(h)$ applied at the terminal cross sections as shown in Fig. 2(a). The bond torque $t(z)$ and the torque $T_0 - T_*(0)$ are assumed to be distributed linearly in the form of eqn (16a) over their respective cross sections $\bar{\pi}_z (0 < z < h)$ and $\bar{\pi}_0$, while the torque $T_*(h)$ in the singular form of eqn (17a) over the cross section $\bar{\pi}_h$.

Conversely, the bond torques and end torques are exerted by the extended half space B on the fictitious bar B_*, which may be treated as a one-dimensional elastic continuum, for which the equation of equilibrium is

$$t(z) = -dT_*(z)/dz \quad (20)$$

and the torque-twist relation of the fictitious bar is

$$T_*(z) = \pi\mu_* \, d\phi_*(z)/2\,dz \quad (21)$$

where $T_*(z)$ and $\phi_*(z)$ are fictitious torque and angle of twist of the bar respectively.

The governing integral equation can be derived using the following compatibility condition between B_* and the edge of region D as

$$d\phi_*(z)/dz = dv(1^-, z)/dz, \quad (0 \leq z \leq h) \tag{22}$$

where $v(r, z)$ is the displacement in θ direction at a point $\mathbf{x}(r, \theta, z)$ in domain B, and 1^- denotes a value infinitesimally less than unity. It should be mentioned that the original compatibility condition proposed in Ref. [6], where it was between B_* and the corresponding average over a cross section of region D, was found not accurate enough by the present authors in a separate calculation. The function $v(r, z)$ can be expressed in the form

$$v(r, z) = [T_0 - T_*(0)]v_T(r, z; 0) + T_*(h)v_T(r, z; h) + \int_0^h v_T(r, z; z')t(z')\,dz' \tag{23}$$

where $v_T(r, z; z')$ is the fundamental solution derived in the previous section, i.e. the displacement in θ direction at a point $\mathbf{x}(r, \theta, z)$ due to a unit torque applied at a depth z' (Fig. 4). Substitution of eqns (20), (21) and (23) in eqn (22) results in,

$$2T_*(z)/\pi\mu_* = [T_0 - T_*(0)]\phi^0_{Tz}(z, 0) + T_*(h)\phi^0_{Tz}(z, h) - \int_0^h \phi^0_{Tz}(z, z')\frac{dT_*(z')}{dz'}\,dz' \tag{24}$$

where $\phi^0_{Tz}(z, z')$ is an influence function defined as

$$\phi^0_{Tz}(z, z') = \partial v_T(1^-, z; z')/\partial z \tag{25}$$

and presented in the Appendix. It should be noted that this influence function is smooth and continuous everywhere except at $z = z'$, where the magnitude of the discontinuity according to eqn (16a) is equal to $2/\pi\mu_1$ for $0 < z < h$. In case of incorporating the stress singularity at the end of the bar, $\phi^0_{Tz}(z, z')$ when $z = z' = h$ diverges due to eqn (17a), thus requires an appropriate handling in the numerical solution scheme.

Integrating the integrals in eqn (24) by parts, while taking proper account of the discontinuity, results in

$$\frac{2T_*(z)}{\pi}\left[\frac{1}{\mu_*} + \frac{1}{\mu_1}\right] - \int_0^h T_*(z')\frac{\partial\phi^0_{Tz}(z, z')}{\partial z'}\,dz' = T_0\phi^0_{Tz}(z, 0). \tag{26}$$

Equation (26) is a Fredholm integral equation of the second kind governing the distribution of $T_*(z)$ along the fictitious bar.

The real bar torque $T(z)$ can be obtained by combining the fictitious torque $T_*(z)$ with the corresponding area integral of the shear stress $\sigma_{\theta z}$ in the region D of B, i.e.

$$T(z) = T_*(z) + \int_{\pi_z} r\sigma_{\theta z}(r, z)\,dA, \quad (0 \leq z \leq h) \tag{27}$$

while the angle of twist of the real bar taken as equal to that of the fictitious bar, in view of eqn (22) can be written as

$$\phi_*(z) = v(1, z), \quad (0 \leq z \leq h). \tag{28}$$

In view of eqn (23), performing appropriate integrations in eqns (27) and (28) leads to, respectively

$$T(z) = T_0\tau^0_{\theta z}(z, 0) + \int_0^h T_*(z')\frac{\partial\tau^0_{\theta z}(z, z')}{\partial z'}\,dz' \tag{29}$$

$$\phi_*(z) = T_0\phi_T{}^0(z, 0) + \int_0^h T_*(z')\frac{\partial\phi_T{}^0(z, z')}{\partial z'}\,dz' \tag{30}$$

where $\tau^0_{\theta z}(z, z')$ and $\phi_T{}^0(z, z')$ are influence functions defined as

$$\tau^0_{\theta z}(z, z') = \int_{\pi_z} r\sigma_{\theta zT}(r, z; z')\,dA \tag{31a}$$

$$\phi_T{}^0(z, z') = v_T(1, z; z') \tag{31b}$$

in which $\sigma_{\theta zT}(r, z; z')$ is a shear stress in the fundamental solution depicted in Fig. 4.

Appendix of this paper contains the listing of the influence functions $\phi^0_{Tz}(z, z')$, $\tau^0_{\theta z}(z, z')$ and $\phi_T{}^0(z, z')$ together with the numerical scheme for integrals involved, which are in the Lipschitz–Hankel type involving products of Bessel functions.

6. NUMERICAL SOLUTION SCHEME

The solution to the Fredholm integral equation governing $T_*(z)$ has to resort to an appropriate numerical method due to the complexity of the kernel $\partial\phi^0_{Tz}(z, z')/\partial z'$, which can be shown to have an integrable logarithamic singularity at $z = z'$. The solution scheme adopted by Hopkins and Hamming[9] and Lee and Rogers[10] in the solution of Volterra integral equations is employed herein: Dividing the interval of integration into n equal partitions and denoting each mesh point by z_j; $j = 1,2,3,\ldots,n+1$, with $z_1 = 0$ and $z_{n+1} = h$, eqn (26) becomes

$$\frac{2T_*(z_i)}{\pi}\left[\frac{1}{\mu_*}+\frac{1}{\mu_1}\right] - \sum_{j=1}^{n}\frac{1}{2}[T_*(z_j)+T_*(z_{j+1})][\phi^0_{Tz}(z_i, z_{j+1}) - \phi^0_{Tz}(z_i, z_j)] = T_0\phi^0_{Tz}(z_i, 0) \tag{32}$$

which is a set of $n+1$ simultaneous equations, the solution of which results in the fictitious torque $T_*(z)$ at all mesh points.

In case of the singularity of the stress field at the base perimeter of the bar, $\phi^0_{Tz}(h, h)$ contains a singular term of the form

$$\int_0^\infty \xi^{-k+(1/2)}J_1(\xi r)J_{k+(3/2)}(\xi)\,d\xi = 2^{(1/2)-k}\frac{r(1-r^2)^{k-(1/2)}}{\Gamma(k+1/2)},\quad (r = 1^-) \tag{33}$$

thus there exists in eqn (32) an indeterminate term $T_*(h)\phi^0_{Tz}(h, h)$. As z tends to h, $T_*(z)$ shall approach zero in the form

$$T_*(z) \sim [1-(z/h)^2]^{(1/2)-k},\quad (z/h \to 1^-). \tag{34}$$

In order to handle this situation in the numerical solution to eqn (32), the numerical value of 1^- in eqn (33) is increased towards unity gradually until $T_*(h)$ is sufficiently close to zero and other essential results become stable. The technique is found to be successful as exemplified in Table 1. Physically, the shear stress along the mantle of the cylindrical bar is directly proportional to the bond torque, i.e. $\sigma_{r\theta}(1, z) \sim t(z)$; thus with the help of eqns (20) and (34) we can confirm the singular form of $\sigma_{r\theta}(1, z)$ as eqn (4b).

7. DISCUSSION OF RESULTS AND CONCLUSIONS

The study of Luco[2] was rigorous but restrictive to the case of rigid bars ($\beta_1 = 0$). The problem was governed by a set of two coupled integral equations, which was solved by an elaborate numerical scheme. Numerical results of the torque-twist angle relationship and the

Table 1. Example of convergence of proposed solution as r approaches 1^-; $h/a = 3$, $\beta_1 = 0$, and $\beta_2 = 1$

$r = 1^-$	$T_*(h)/T_0$	$T(h)/T_0$	$3T_0/16\mu_s a^3\phi_*(0)$
0.95	0.081	0.110	8.48
0.99	0.048	0.106	8.47
0.995	0.024	0.100	8.46
0.9975	0.008	0.100	8.45

Table 2. $3T_0/16\mu_3 a^3\phi_*(0)$ for rigid bars ($\beta_1 = 0$) in comparison with Luco's results—values in parenthesis being computed by Luco's approximate formula, eqn (35)

h/a	$\beta_2 = 1$		$\beta_2 = 0.75$		$\beta_2 = 0.50$		$\beta_2 = 0.25$	
	Proposed	Luco [2]	Proposed	Luco [2]	Proposed	Luco [2]	Proposed	Luco [2]
1	3.51	3.73 (3.36)	2.92	3.08 (2.77)	2.20	2.42 (2.18)	1.36	1.73 (1.59)
2	6.04	6.14 (5.71)	4.80	4.90 (4.53)	3.55	3.64 (3.36)	2.20	2.35 (2.18)
3	8.45	8.53 (8.07)	6.60	6.70 (6.30)	4.82	4.84 (4.53)	2.88	2.95 (2.77)
4	10.84	10.90 (10.42)	8.43	8.48 (8.07)	5.98	6.03 (5.71)	3.44	3.55 (3.36)

Table 3. $T(h)/T_0$ for rigid bars ($\beta_1 = 0$) in comparison with Luco's results

h/a	$\beta_2 = 1$		$\beta_2 = 0.75$		$\beta_2 = 0.50$		$\beta_2 = 0.25$	
	Proposed	Luco [2]	Proposed	Luco [2]	Proposed	Luco [2]	Proposed	Luco [2]
1	0.24	0.19	0.29	0.24	0.37	0.32	0.56	0.49
2	0.14	0.11	0.18	0.15	0.25	0.21	0.39	0.36
3	0.10	0.08	0.12	0.11	0.19	0.16	0.29	0.29
4	0.07	0.06	0.10	0.09	0.13	0.13	0.24	0.24

torque transfer to the lower layer of the half space was obtained for h/a ratio up to 4, and an approximate formula for the torque-twist angle relationship was proposed as

$$T_0 = \frac{16}{3}\mu_3 a^3 \phi_*(0)\left[1 + \frac{3}{4}\pi\beta_2 h/a\right]. \tag{35}$$

Inside the brackets above, the first term is the solution to the problem of a torque applied on the surface of a homogeneous elastic half space, and the second term is the torsion of a rigid core completely embedded in a free-free plate of thickness h. In comparison with the exact results, this formula is accurate, though by its nature always gives a higher twist angle for a prescribed T_0.

The present study is applicable to an elastic bar as well as a rigid one, and governed by a single integral equation. Thus it is relatively simpler to obtain numerical results for any values of the three parameters involved β_1, β_2 and h/a ratio. The accuracy of the method is shown in Tables 2 and 3, in which the results are compared with those by Luco[2] for $h/a = 1$ to 4. It can be seen that the agreement between two approaches is good and becomes better as the bar length increases. The latter point is natural due to the assumption in the present approach of the fictitious bar as a one-dimensional elastic continuum, which should be more true as the bar length increases. As should be expected, the approximate formula by Luco[2], eqn (35), gives lowest results in Table 2 excepting for a very short bar ($h/a = 1$).

Tables 4–7 contain numerical results of the torque-twist angle relationship and the torque at the lower end of the bar for h/a ratio as big as 100. Furthermore, these tables show a comparison of cases with singular and non-singular stress conditions along the base perimeter of the bar. It can be noted that the effect of the singular stress condition is not so significant, especially for long bars and when the main concern is on the relationship between the applied torque T_0 and the angle of twist of the top end of the bar $\phi_*(0)$. This type of situation is more pronounced in the problem of a flexible bar (Tables 6 and 7). It should be mentioned also that the case of non-singular stress condition involves less computational efforts. As should be expected, the approximate formula by Luco[2] gives lowest results in Table 4 excepting for a very short bar ($h/a = 1$).

Table 4. $3T_0/16\mu_3 a^3\phi_*(0)$ of cases with singular and non-singular stress conditions along base perimeter of the rigid bar ($\beta_1 = 0$)—values in parentheses being computed by Luco's approximate formula, eqn (35)

h/a	$\beta_2 = 1$		$\beta_2 = 0.75$		$\beta_2 = 0.50$		$\beta_2 = 0.25$	
	Singular	Non-Singular	Singular	Non-Singular	Singular	Non-Singular	Singular	Non-Singular
1	3.51	3.46 (3.36)	2.92	2.87 (2.77)	2.20	2.16 (2.18)	1.36	1.30 (1.59)
2	6.04	6.09 (5.71)	4.80	4.84 (4.53)	3.55	3.60 (3.36)	2.20	2.24 (2.18)
3	8.45	8.50 (8.07)	6.60	6.68 (6.30)	4.82	4.91 (4.53)	2.88	3.13 (2.77)
4	10.84	10.90 (10.42)	8.43	8.51 (8.07)	5.98	6.12 (5.71)	3.44	3.74 (3.36)
10	24.88	25.08 (24.56)	18.98	19.23 (18.67)	13.10	13.34 (12.78)	6.96	7.25 (6.89)
20	48.44	48.69 (48.12)	36.65	36.92 (36.34)	24.88	25.10 (24.56)	12.85	13.14 (12.78)
50	119.12	119.41 (118.81)	89.66	90.04 (89.36)	60.22	60.68 (59.90)	30.52	30.96 (30.45)
100	236.93	237.42 (236.62)	178.02	178.56 (177.71)	119.13	119.62 (118.81)	59.97	60.39 (59.90)

Table 5. $T(h)/T_0$ of cases with singular and non-singular stress conditions along base perimeter of the bar; $\beta_1 = 0$

h/a	$\beta_2 = 1$		$\beta_2 = 0.75$		$\beta_2 = 0.50$		$\beta_2 = 0.25$	
	Singular	Non-Singular	Singular	Non-Singular	Singular	Non-Singular	Singular	Non-Singular
1	0.24	0.33	0.29	0.37	0.37	0.42	0.56	0.58
2	0.14	0.20	0.18	0.24	0.25	0.28	0.39	0.40
3	0.10	0.15	0.12	0.17	0.19	0.21	0.29	0.31
4	0.07	0.11	0.10	0.14	0.13	0.17	0.24	0.26
10	0.03	0.05	0.04	0.06	0.05	0.08	0.09	0.12
20	0.01	0.02	0.02	0.03	0.03	0.04	0.04	0.06
50	0.004	0.010	0.005	0.014	0.006	0.018	0.010	0.027
100	0.002	0.008	0.002	0.010	0.003	0.011	0.005	0.017

Table 6. $3T_0/16\mu_3 a^3\phi_*(0)$ of cases with singular and non-singular stress conditions along base perimeter of the bar; $\beta_1 = 0.1$

h/a	$\beta_2 = 1$		$\beta_2 = 0.75$	$\beta_2 = 0.50$	$\beta_2 = 0.25$
	Singular	Non-Singular	No singularity exists.	No singularity exists.	No singularity exists.
1	2.47	2.46	1.91	1.31	0.72
2	2.86	2.86	2.15	1.44	0.73
3	2.96	2.96	2.18	1.47	0.74
4	2.98	2.98	2.22	1.48	0.74
10	3.02	3.02	2.26	1.51	0.75
20	3.02	3.02	2.26	1.51	0.76
50	3.02	3.02	2.26	1.51	0.76
100	3.02	3.02	2.26	1.51	0.76

Table 7. $T(h)/T_0$ of cases with singular and non-singular stress conditions along base perimeter of the bar; $\beta_1 = 0.1$

h/a	$\beta_2 = 1$		$\beta_2 = 0.75$	$\beta_2 = 0.50$	$\beta_2 = 0.25$
	Singular	Non-Singular	No singularity exists.	No singularity exists.	No singularity exists.
1	0.19	0.24	0.27	0.28	0.38
2	0.07	0.10	0.11	0.13	0.15
3	0.03	0.04	0.05	0.06	0.06
4	0.01	0.02	0.02	0.03	0.03
10	0.000	0.000	0.000	0.001	0.001
20	0.000	0.000	0.000	0.000	0.000
50	0.000	0.000	0.000	0.000	0.000
100	0.000	0.000	0.000	0.000	0.000

The significance of the flexibility of the bar can be obviously seen by comparing the results of the twist angle in Table 6 with those in Tables 2 and 4. In addition, Table 6 shows that an elastic bar with the length greater than a certain value can be treated as an infinitely long bar. We may estimate a twist angle for the case of an infinitely long bar ($h/a = \infty$). and a homogeneous half space ($\beta_2 = 1$) from a graph in Ref. [4], by substracting the twist angle due to the St. Venant's torsion of the unembedded part of the bar from the result given by the graph. In doing so for $\beta_1 = 0.1$, the value of $3T_0/16\mu_3 a^3\phi_*(0)$ is 3.03 comparing with the value 3.02 obtained by the present study for $h/a = 10$ to 100.

REFERENCES

1. M. L. Williams, Stress singularities resulting from various boundary conditions in angular corners of plates in extension. *J. Appl. Mech. ASME* **19**, 526 (1952).
2. J. E. Luco, Torsion of a rigid cylinder embedded in an elastic half space. *J. Appl. Mech. ASME* **43**, 419 (1976).
3. N. J. Freeman and L. M. Keer, Torsion of a cylindrical rod welded to an elastic half space. *J. Appl. Mech. ASME* **34**, 687 (1967).
4. L. M. Keer and N. J. Freeman, Load transfer problem for an embedded shaft in torsion. *J. Appl. Mech. ASME* **37**, 959 (1970).
5. V. K. Luk and L. M. Keer, Stress analysis of an elastic half space containing an axially-loaded rigid cylindrical rod. *Int. J. Solids Structures* **10**, 1179 (1979).
6. R. Muki and E. Sternberg, Elastostatic load-transfer to a half space from a partially embedded axially loaded rod. *Int. J. Solids Structures* **6**, 69 (1970).
7. E. Reissner and H. F. Sagoci, Forced torsional oscillations of an elastic half space. *J. Appl. Phys.* **15**, 652 (1944).
8. R. Muki, Asymmetric problems of the theory of elasticity for a semi-infinite solid and a thick plate *Progress in Solid Mechanics* (Edited by I. N. Sneddon and R. Hill), Vol. 1, p. 399. North Holland, Amsterdam (1960).
9. I. L. Hopkins and R. W. Hamming, On creep and relaxation. *J. Appl. Phys.* **28**, 906 (1957).
10. E. H. Lee and T. G. Roger, Solution of viscoelastic stress analysis problems using measured creep and relaxation functions. *J. Appl. Mech. ASME* **30**, 127 (1963).
11. G. Eason, B. Noble and I. N. Sneddon, On certain integrals of Lipschitz-Hankel type involving products of Bessel functions. *Phil. Trans. R. Soc. London* **A247**, 529 (1955).
12. K. S. Chan, P. Karasudhi and S. L. Lee, Force at a point in the interior of a layered elastic half space. *Int. J. Solids Structures* **10**, 1179 (1974).
13. M. Abramowitz and I. A. Stegun, *Handbook of Mathematical Functions*, pp. 360, 369, 379, 886. Dover, New York (1972).

APPENDIX

Influence functions

The influence function $\phi^0_{Tz}(z, z')$ defined in eqn (25) can be expressed as follows

$$\phi^0_{Tz}(z, z') = -\frac{1}{\pi\mu_1(1+\mu_0)}\int_0^\infty \frac{J_1(1^-\xi)J_2(\xi)}{H(\xi h)}\left\{(1+\mu_0)\left[\frac{|z'-z|}{(z'-z)}e^{-\xi|z'-z|} - e^{-\xi(z+z')}\right] + (1-\mu_0)\left[e^{-\xi(2h-z'-z)} - \frac{|z'-z|}{(z'-z)}e^{-\xi(2h-|z'-z|)}\right]\right\}d\xi \quad (z \neq z) \tag{36}$$

where

$$H(\xi h) = (1+\mu_0 - e^{-2\xi h} + \mu_0 e^{-2\xi h})/(1+\mu_0) \tag{37}$$

$$\mu_0 = \mu_3/\mu_1 = \beta_2^{-1}. \tag{38}$$

When singular stress condition exists along the base perimeter of the bar,

$$\phi^0_{Tz}(z,h) = -\frac{(k+1/2)(k+3/2)}{\pi\mu_1(1+\mu_0)} 2^{k-1/2}\Gamma(k+1/2)\int_0^\infty \frac{J_1(1^-\xi)}{H(\xi h)} J_{k+3/2}(\xi)\xi^{-k+1/2} \times [e^{-\xi(h-z)} - e^{-\xi(h+z)}]\,d\xi, \quad (0 \le z < h). \tag{39}$$

The influence function $\tau^0_{\theta z}(z,z')$ defined in eqn (31a) can be expressed as follows,

$$\tau^0_{\theta z}(z,z') = -2\int_0^\infty \frac{J_2^2(\xi)}{H(\xi h)(1+\mu_0)\xi}\left\{(1+\mu_0)\left[\frac{|z'-z|}{(z'-z)} e^{-\xi|z'-z|} - e^{-\xi(z+z')}\right] + (1-\mu_0)\left[e^{-\xi(2h-z'-z)} - \frac{|z'-z|}{(z'-z)} e^{-\xi(2h-|z'-z|)}\right]\right\} d\xi, \quad (z \ne z') \tag{40}$$

When singular stress condition exists along the base perimeter of the bar,

$$\tau^0_{\theta z}(z,h) = 2^{k+1/2}(k+1/2)(k+3/2)\Gamma(k+1/2)\int_0^\infty \frac{\xi^{-k-1/2}J_2(\xi)}{H(\xi h)(1+\mu_0)} J_{k+3/2}(\xi) \times [e^{-\xi(h-z)} - e^{-\xi(h+z)}]\,d\xi, \quad (0 \le z \le h). \tag{41}$$

The influence function $\phi_T{}^0(z,z')$ defined in eqn (31b) can be expressed as follows

$$\phi_T{}^0(z,z') = -\frac{1}{\pi\mu_1(1+\mu_0)}\int_0^\infty \frac{J_1(\xi)J_2(\xi)}{\xi H(\xi h)}\{(1+\mu_0)[e^{-\xi|z'-z|} + e^{-\xi(z'+z)}] + (1-\mu_0)[e^{-\xi(2h-|z'-z|)} + e^{-\xi(2h-z'-z)}]\}\,d\xi, \quad (z \ne z'). \tag{42}$$

When singular stress condition exists along the base perimeter of the bar,

$$\phi_T{}^0(z,h) = -2^{k-1/2}\frac{(k+1/2)(k+3/2)}{\pi\mu_1(1+\mu_0)}\Gamma(k+1/2)\int_0^\infty \frac{\xi^{-k-1/2}J_1(\xi)}{H(\xi h)} J_{k+3/2}(\xi) \times [e^{-\xi(h-z)} + e^{-\xi(h+z)}]\,d\xi, \quad (0 \le z \le h). \tag{43}$$

Numerical scheme for infinite integrals involved

Infinite integrals appearing in eqns (36) and (39)–(43) can be put in the Lipschitz–Hankel form[11] by approximating accurately the common denominator $H(\xi h)$ by a set of exponential terms as suggested by Chan, Karasudhi and Lee[12]. For examples; for $\mu_0 = 0.5$,

$$1/H(\xi h) = 1 + 0.3328\,e^{-2\xi h} + 0.1162\,e^{-4\xi h} + 0.0207\,e^{-6\xi h} + 0.0302\,e^{-8\xi h} \tag{44}$$

for

$$\mu_0 = 5.0,$$
$$1/H(\xi h) = 1 - 0.6647\,e^{-2\xi h} + 0.4219\,e^{-4\xi h} - 0.212\,e^{-6\xi h} + 0.0549\,e^{-8\xi h} \tag{45}$$

anf for

$$\mu_0 = \infty,$$
$$1/H(\xi h) = 1 - 0.9909\,e^{-2\xi h} + 0.8915\,e^{-4\xi h} - 0.5695\,e^{-6\xi h} + 0.1689\,e^{-8\xi h}. \tag{46}$$

It should be noted also that $1/H(\xi h)$ for $\mu_0 = 1$ is identical to unity.

Consequently, the influence functions involve integrals of the form

$$J(\mu,\omega;\lambda) = \int_0^\infty J_\mu(\xi)J_\nu(\rho\xi)\,e^{-\omega\xi}\xi^\lambda\,d\xi. \tag{47}$$

Eason *et al.*[11] showed that these integrals are convergent for $\eta > 0$ if $\mu + \nu + \lambda > -1$, and for $\eta = 0$ if

$$\mu + \nu + 1 > -\lambda > -1 \text{ for } \rho \ne 1 \tag{48a}$$

$$\mu + \nu + 1 > -\lambda > 0 \text{ for } \rho = 1. \tag{48b}$$

All individual infinite integrals in the influence functions are convergent according to the above criteria except the term eqn (33) in the influence function $\phi^0_{Tz}(h,h)$ which diverges. For the convergent integrals, it is found that the most efficient numerical scheme is the direct integration by means of the extended Simpson's rule[13]. The numerical values of Bessel functions with integer orders are computed from approximate closed form formulae, while those with fractional orders from an integral formula[13]. The results, obtained by using 70 (instead of ∞) as the upper limit and 0.1 as the increment of the integration, agree very closely with those tabulated in Ref.[11].